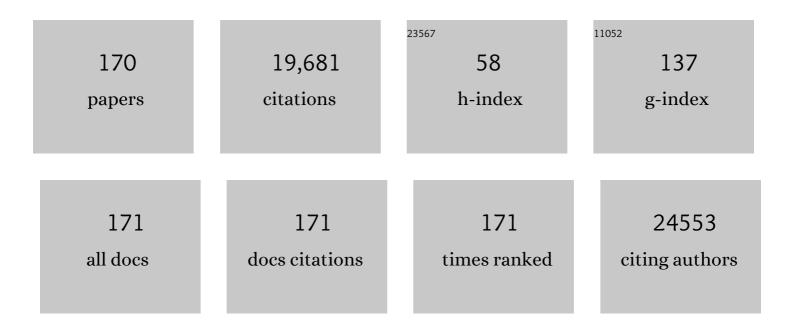
## Qing Zhang

List of Publications by Year in descending order

Source: https://exaly.com/author-pdf/868442/publications.pdf Version: 2024-02-01



#	Article	IF	CITATIONS
1	From Bulk to Monolayer MoS <sub>2</sub> : Evolution of Raman Scattering. Advanced Functional Materials, 2012, 22, 1385-1390.	14.9	3,354
2	Single-Layer MoS <sub>2</sub> Phototransistors. ACS Nano, 2012, 6, 74-80.	14.6	3,103
3	High phase-purity 1T′-MoS2- and 1T′-MoSe2-layered crystals. Nature Chemistry, 2018, 10, 638-643.	13.6	757
4	Room-Temperature Near-Infrared High-Q Perovskite Whispering-Gallery Planar Nanolasers. Nano Letters, 2014, 14, 5995-6001.	9.1	702
5	Highâ€Quality Whisperingâ€Galleryâ€Mode Lasing from Cesium Lead Halide Perovskite Nanoplatelets. Advanced Functional Materials, 2016, 26, 6238-6245.	14.9	529
6	Topological polaritons and photonic magic angles in twisted α-MoO3 bilayers. Nature, 2020, 582, 209-213.	27.8	413
7	Vapor Phase Synthesis of Organometal Halide Perovskite Nanowires for Tunable Room-Temperature Nanolasers. Nano Letters, 2015, 15, 4571-4577.	9.1	405
8	Synthesis of Organic–Inorganic Lead Halide Perovskite Nanoplatelets: Towards Highâ€Performance Perovskite Solar Cells and Optoelectronic Devices. Advanced Optical Materials, 2014, 2, 838-844.	7.3	363
9	High-Efficiency Light-Emitting Diodes of Organometal Halide Perovskite Amorphous Nanoparticles. ACS Nano, 2016, 10, 6623-6630.	14.6	347
10	Batch production of 6-inch uniform monolayer molybdenum disulfide catalyzed by sodium in glass. Nature Communications, 2018, 9, 979.	12.8	338
11	Chemical Reduction of Intrinsic Defects in Thicker Heterojunction Planar Perovskite Solar Cells. Advanced Materials, 2017, 29, 1606774.	21.0	318
12	Raman spectroscopy of atomically thin two-dimensional magnetic iron phosphorus trisulfide (FePS) Tj ETQq0 0 0	rgβŢ /Ove 4.4	rlock 10 Tf 5
13	A room temperature low-threshold ultraviolet plasmonic nanolaser. Nature Communications, 2014, 5, 4953.	12.8	278

14	Advances in Small Perovskiteâ $\in$ Based Lasers. Small Methods, 2017, 1, 1700163.	8.6	268
15	Chemical alterations taken place during deep-fat frying based on certain reaction products: A review. Chemistry and Physics of Lipids, 2012, 165, 662-681.	3.2	267
16	Metal halide perovskite nanomaterials: synthesis and applications. Chemical Science, 2017, 8, 2522-2536.	7.4	233
17	Halide Perovskite Semiconductor Lasers: Materials, Cavity Design, and Low Threshold. Nano Letters, 2021, 21, 1903-1914.	9.1	220
18	Vertically Aligned Gold Nanorod Monolayer on Arbitrary Substrates: Self-Assembly and Femtomolar Detection of Food Contaminants. ACS Nano, 2013, 7, 5993-6000.	14.6	218

#	Article	IF	CITATIONS
19	Flexible Visible–Infrared Metamaterials and Their Applications in Highly Sensitive Chemical and Biological Sensing. Nano Letters, 2011, 11, 3232-3238.	9.1	215
20	3R MoS <sub>2</sub> with Broken Inversion Symmetry: A Promising Ultrathin Nonlinear Optical Device. Advanced Materials, 2017, 29, 1701486.	21.0	197
21	Two-dimensional metallic tantalum disulfide as a hydrogen evolution catalyst. Nature Communications, 2017, 8, 958.	12.8	191
22	Solution-processed highly bright and durable cesium lead halide perovskite light-emitting diodes. Nanoscale, 2016, 8, 18021-18026.	5.6	160
23	Unveiling Structurally Engineered Carrier Dynamics in Hybrid Quasi-Two-Dimensional Perovskite Thin Films toward Controllable Emission. Journal of Physical Chemistry Letters, 2017, 8, 4431-4438.	4.6	147
24	Wavelength Tunable Single Nanowire Lasers Based on Surface Plasmon Polariton Enhanced Burstein–Moss Effect. Nano Letters, 2013, 13, 5336-5343.	9.1	145
25	Strong Exciton–Photon Coupling and Lasing Behavior in All-Inorganic CsPbBr <sub>3</sub> Micro/Nanowire Fabry-Pérot Cavity. ACS Photonics, 2018, 5, 2051-2059.	6.6	145
26	Role of the Exciton–Polariton in a Continuous-Wave Optically Pumped CsPbBr <sub>3</sub> Perovskite Laser. Nano Letters, 2020, 20, 6636-6643.	9.1	145
27	Recent developments and future directions in the growth of nanostructures by van der Waals epitaxy. Nanoscale, 2013, 5, 3570.	5.6	144
28	Interface nano-optics with van der Waals polaritons. Nature, 2021, 597, 187-195.	27.8	143
29	Effect of High Hydrostatic Pressure on Physicochemical and Structural Properties of Rice Starch. Food and Bioprocess Technology, 2012, 5, 2233-2241.	4.7	141
30	Ultrathin CsPbX <sub>3</sub> Nanowire Arrays with Strong Emission Anisotropy. Advanced Materials, 2018, 30, e1801805.	21.0	135
31	Tailoring the Lasing Modes in Semiconductor Nanowire Cavities Using Intrinsic Self-Absorption. Nano Letters, 2013, 13, 1080-1085.	9.1	133
32	Surface Plasmon Enhanced Strong Exciton–Photon Coupling in Hybrid Inorganic–Organic Perovskite Nanowires. Nano Letters, 2018, 18, 3335-3343.	9.1	133
33	Authentication of edible vegetable oils adulterated with used frying oil by Fourier Transform Infrared Spectroscopy. Food Chemistry, 2012, 132, 1607-1613.	8.2	132
34	Lasing from Mechanically Exfoliated 2D Homologous Ruddlesden–Popper Perovskite Engineered by Inorganic Layer Thickness. Advanced Materials, 2019, 31, e1903030.	21.0	128
35	Whispering Gallery Mode Lasing from Hexagonal Shaped Layered Lead Iodide Crystals. ACS Nano, 2015, 9, 687-695.	14.6	118
36	Strong Exciton–Photon Coupling in Hybrid Inorganic–Organic Perovskite Micro/Nanowires. Advanced Optical Materials, 2018, 6, 1701032.	7.3	114

#	Article	IF	CITATIONS
37	Controlled Growth and Thicknessâ€Dependent Conductionâ€Type Transition of 2D Ferrimagnetic Cr <sub>2</sub> S <sub>3</sub> Semiconductors. Advanced Materials, 2020, 32, e1905896.	21.0	114
38	Large-Scale Thin CsPbBr <sub>3</sub> Single-Crystal Film Grown on Sapphire <i>via</i> Chemical Vapor Deposition: Toward Laser Array Application. ACS Nano, 2020, 14, 15605-15615.	14.6	112
39	Perovskite semiconductors for room-temperature exciton-polaritonics. Nature Materials, 2021, 20, 1315-1324.	27.5	109
40	Allâ€Inorganic CsPbBr <sub>3</sub> Nanowire Based Plasmonic Lasers. Advanced Optical Materials, 2018, 6, 1800674.	7.3	107
41	Atomically Dispersed Co–P <sub>3</sub> on CdS Nanorods with Electronâ€Rich Feature Boosts Photocatalysis. Advanced Materials, 2020, 32, e1904249.	21.0	105
42	Tuning Gold Nanorod-Nanoparticle Hybrids into Plasmonic Fano Resonance for Dramatically Enhanced Light Emission and Transmission. Nano Letters, 2011, 11, 49-55.	9.1	104
43	Epitaxial Growth of Two-Dimensional Metal–Semiconductor Transition-Metal Dichalcogenide Vertical Stacks (VSe <sub>2</sub> /MX <sub>2</sub> ) and Their Band Alignments. ACS Nano, 2019, 13, 885-893.	14.6	102
44	Multiple Magnetic Mode-Based Fano Resonance in Split-Ring Resonator/Disk Nanocavities. ACS Nano, 2013, 7, 11071-11078.	14.6	97
45	Perovskite quantum dot lasers. InformaÄnÃ-Materiály, 2020, 2, 170-183.	17.3	97
46	Direct Chemical Vapor Deposition Growth and Band-Gap Characterization of MoS <sub>2</sub> / <i>h</i> -BN van der Waals Heterostructures on Au Foils. ACS Nano, 2017, 11, 4328-4336.	14.6	87
47	Discrimination of Edible Vegetable Oil Adulteration with Used Frying Oil by Low Field Nuclear Magnetic Resonance. Food and Bioprocess Technology, 2013, 6, 2562-2570.	4.7	81
48	Observation of Selective Plasmon-Exciton Coupling in Nonradiative Energy Transfer: Donor-Selective versus Acceptor-Selective Plexcitons. Nano Letters, 2013, 13, 3065-3072.	9.1	77
49	Vertical 1Tâ€₹aS <sub>2</sub> Synthesis on Nanoporous Gold for Highâ€Performance Electrocatalytic Applications. Advanced Materials, 2018, 30, e1705916.	21.0	75
50	Ultrafast Charge Transfer in Perovskite Nanowire/2D Transition Metal Dichalcogenide Heterostructures. Journal of Physical Chemistry Letters, 2018, 9, 1655-1662.	4.6	75
51	In situ Raman spectroscopy of topological insulator Bi2Te3 films with varying thickness. Nano Research, 2013, 6, 688-692.	10.4	72
52	Fluorophore-Doped Core–Multishell Spherical Plasmonic Nanocavities: Resonant Energy Transfer toward a Loss Compensation. ACS Nano, 2012, 6, 6250-6259.	14.6	71
53	Unveiling lasing mechanism in CsPbBr <sub>3</sub> microsphere cavities. Nanoscale, 2019, 11, 3145-3153.	5.6	71
54	Compositionâ€Tunable Vertically Aligned CdS <sub><i>x</i></sub> Se <sub>1â€<i>x</i></sub> Nanowire Arrays via van der Waals Epitaxy: Investigation of Optical Properties and Photocatalytic Behavior. Advanced Materials, 2012, 24, 4151-4156.	21.0	69

#	Article	IF	CITATIONS
55	Excitonics of semiconductor quantum dots and wires for lighting and displays. Laser and Photonics Reviews, 2014, 8, 73-93.	8.7	67
56	Edge-oriented and steerable hyperbolic polaritons in anisotropic van der Waals nanocavities. Nature Communications, 2020, 11, 6086.	12.8	67
57	Chemical Vapor Deposition Grown Waferâ€Scale 2D Tantalum Diselenide with Robust Chargeâ€Densityâ€Wave Order. Advanced Materials, 2018, 30, e1804616.	21.0	63
58	Electric-Field-Dependent Photoconductivity in CdS Nanowires and Nanobelts: Exciton Ionization, Franz–Keldysh, and Stark Effects. Nano Letters, 2012, 12, 2993-2999.	9.1	62
59	Fabry–Pérot Oscillation and Room Temperature Lasing in Perovskite Cube orner Pyramid Cavities. Small, 2018, 14, 1703136.	10.0	61
60	Recent Progress of Strong Exciton–Photon Coupling in Lead Halide Perovskites. Advanced Materials, 2019, 31, e1804894.	21.0	60
61	Vapor-Phase Incommensurate Heteroepitaxy of Oriented Single-Crystal CsPbBr <sub>3</sub> on GaN: Toward Integrated Optoelectronic Applications. ACS Nano, 2019, 13, 10085-10094.	14.6	59
62	Temperature-dependent photoluminescence and lasing properties of CsPbBr3 nanowires. Applied Physics Letters, 2019, 114, .	3.3	59
63	Direct synthesis and in situ characterization of monolayer parallelogrammic rhenium diselenide on gold foil. Communications Chemistry, 2018, 1, .	4.5	58
64	Full-color enhanced second harmonic generation using rainbow trapping in ultrathin hyperbolic metamaterials. Nature Communications, 2021, 12, 6425.	12.8	58
65	Scalable Production of Two-Dimensional Metallic Transition Metal Dichalcogenide Nanosheet Powders Using NaCl Templates toward Electrocatalytic Applications. Journal of the American Chemical Society, 2019, 141, 18694-18703.	13.7	56
66	Enhanced Optical Absorption and Slowed Light of Reduced-Dimensional CsPbBr <sub>3</sub> Nanowire Crystal by Exciton–Polariton. Nano Letters, 2020, 20, 1023-1032.	9.1	55
67	Quantum dots on vertically aligned gold nanorod monolayer: plasmon enhanced fluorescence. Nanoscale, 2014, 6, 5592-5598.	5.6	53
68	Epitaxial II–VI Tripod Nanocrystals: A Generalization of van der Waals Epitaxy for Nonplanar Polytypic Nanoarchitectures. ACS Nano, 2012, 6, 2281-2288.	14.6	52
69	Size-Dependent Exciton Recombination Dynamics in Single CdS Nanowires beyond the Quantum Confinement Regime. Journal of Physical Chemistry C, 2013, 117, 10716-10722.	3.1	52
70	Unraveling the Growth of Hierarchical Quasi-2D/3D Perovskite and Carrier Dynamics. Journal of Physical Chemistry Letters, 2018, 9, 1124-1132.	4.6	52
71	Plasmonic Nanolasers in On-Chip Light Sources: Prospects and Challenges. ACS Nano, 2020, 14, 14375-14390.	14.6	52
72	Anisotropic Growth and Scanning Tunneling Microscopy Identification of Ultrathin Even‣ayered PdSe <sub>2</sub> Ribbons, Small, 2019, 15, e1902789.	10.0	50

#	Article	IF	CITATIONS
73	Transparent free-standing metamaterials and their applications in surface-enhanced Raman scattering. Nanoscale, 2014, 6, 132-139.	5.6	48
74	Unambiguous Identification of Carbon Location on the N Site in Semi-insulating GaN. Physical Review Letters, 2018, 121, 145505.	7.8	45
75	High-Temperature Continuous-Wave Pumped Lasing from Large-Area Monolayer Semiconductors Grown by Chemical Vapor Deposition. ACS Nano, 2018, 12, 9390-9396.	14.6	44
76	Highly Enhanced Exciton Recombination Rate by Strong Electron–Phonon Coupling in Single ZnTe Nanobelt. Nano Letters, 2012, 12, 6420-6427.	9.1	43
77	Microstructure evolution of Al–12Si–CuNiMg alloy under high temperature low cycle fatigue. Materials Science & Engineering A: Structural Materials: Properties, Microstructure and Processing, 2013, 574, 186-190.	5.6	43
78	Cooperative Enhancement of Second-Harmonic Generation from a Single CdS Nanobelt-Hybrid Plasmonic Structure. ACS Nano, 2015, 9, 5018-5026.	14.6	43
79	Resolved-sideband Raman cooling of an optical phonon in semiconductor materials. Nature Photonics, 2016, 10, 600-605.	31.4	42
80	Continuousâ€Wave Pumped Perovskite Lasers. Advanced Optical Materials, 2019, 7, 1900544.	7.3	42
81	Phononâ€Assisted Antiâ€Stokes Lasing in ZnTe Nanoribbons. Advanced Materials, 2016, 28, 276-283.	21.0	41
82	Twisted-Angle-Dependent Optical Behaviors of Intralayer Excitons and Trions in WS <sub>2</sub> /WSe <sub>2</sub> Heterostructure. ACS Photonics, 2019, 6, 3082-3091.	6.6	41
83	Semiconductor nanowire plasmonic lasers. Nanophotonics, 2019, 8, 2091-2110.	6.0	40
84	Deep subwavelength fourfold rotationally symmetric split-ring-resonator metamaterials for highly sensitive and robust biosensing platform. Scientific Reports, 2013, 3, 2437.	3.3	38
85	Room temperature continuous-wave excited biexciton emission in perovskite nanoplatelets via plasmonic nonlinear fano resonance. Communications Physics, 2019, 2, .	5.3	36
86	Trapped Exciton–Polariton Condensate by Spatial Confinement in a Perovskite Microcavity. ACS Photonics, 2020, 7, 327-337.	6.6	36
87	Enhanced Trion Emission and Carrier Dynamics in Monolayer WS <sub>2</sub> Coupled with Plasmonic Nanocavity. Advanced Optical Materials, 2020, 8, 2001147.	7.3	36
88	Strong exciton-photon interaction and lasing of two-dimensional transition metal dichalcogenide semiconductors. Nano Research, 2021, 14, 1937-1954.	10.4	36
89	Atomic-scale imaging of CH3NH3PbI3 structure and its decomposition pathway. Nature Communications, 2021, 12, 5516.	12.8	36
90	Tuning Excitonic Properties of Monolayer MoS <sub>2</sub> with Microsphere Cavity by Highâ€Throughput Chemical Vapor Deposition Method. Small, 2017, 13, 1701694.	10.0	35

#	Article	IF	CITATIONS
91	Surfaceâ€Plasmonâ€Assisted Metal Halide Perovskite Small Lasers. Advanced Optical Materials, 2019, 7, 1900279.	7.3	35
92	High Optical Gain of Solutionâ€Processed Mixedâ€Cation CsPbBr <sub>3</sub> Thin Films towards Enhanced Amplified Spontaneous Emission. Advanced Functional Materials, 2021, 31, 2102210.	14.9	35
93	Modulating Resonance Modes and <i>Q</i> Value of a CdS Nanowire Cavity by Single Ag Nanoparticles. Nano Letters, 2011, 11, 4270-4274.	9.1	33
94	Elucidating the Localized Plasmonic Enhancement Effects from a Single Ag Nanowire in Organic Solar Cells. ACS Nano, 2014, 8, 10101-10110.	14.6	33
95	Strain-Modulated Photoelectric Responses from a Flexible α-In2Se3/3R MoS2 Heterojunction. Nano-Micro Letters, 2021, 13, 74.	27.0	31
96	Solvent Recrystallizationâ€Enabled Green Amplified Spontaneous Emissions with an Ultra‣ow Threshold from Pinholeâ€Free Perovskite Films. Advanced Functional Materials, 2021, 31, 2106108.	14.9	31
97	Wavelength Tunable Plasmonic Lasers Based on Intrinsic Self-Absorption of Gain Material. ACS Photonics, 2017, 4, 2789-2796.	6.6	30
98	Analysis of photoluminescence behavior of high-quality single-layer MoS2. Nano Research, 2019, 12, 1619-1624.	10.4	30
99	Two-In-One Method for Graphene Transfer: Simplified Fabrication Process for Organic Light-Emitting Diodes. ACS Applied Materials & Interfaces, 2018, 10, 7289-7295.	8.0	29
100	All Optical Switching through Anistropic Gain of CsPbBr <sub>3</sub> Single Crystal Microplatelet. Nano Letters, 2022, 22, 4049-4057.	9.1	29
101	Solution phase van der Waals epitaxy of ZnO wire arrays. Nanoscale, 2013, 5, 7242.	5.6	27
102	Monitoring of thermal behavior and decomposition products of soybean oil. Journal of Thermal Analysis and Calorimetry, 2014, 115, 19-29.	3.6	26
103	Efficient Quantum Dot Light-Emitting Diodes Based on Trioctylphosphine Oxide-Passivated Organometallic Halide Perovskites. ACS Omega, 2019, 4, 9150-9159.	3.5	26
104	Highâ€ŧemperature low ycle fatigue behaviour of a cast Al–12Si–CuNiMg alloy. Fatigue and Fracture of Engineering Materials and Structures, 2013, 36, 623-630.	3.4	25
105	Subâ€100â€nm Sized Silver Split Ring Resonator Metamaterials with Fundamental Magnetic Resonance in the Middle Visible Spectrum. Advanced Optical Materials, 2014, 2, 280-285.	7.3	25
106	Identifying the Non-Identical Outermost Selenium Atoms and Invariable Band Gaps across the Grain Boundary of Anisotropic Rhenium Diselenide. ACS Nano, 2018, 12, 10095-10103.	14.6	25
107	Highâ€Quality Hexagonal Nonlayered CdS Nanoplatelets for Lowâ€Threshold Whisperingâ€Galleryâ€Mode Lasing. Small, 2019, 15, e1901364.	10.0	24
108	Controlled Gas Molecules Doping of Monolayer MoS <sub>2</sub> via Atomic-Layer-Deposited Al <sub>2</sub> O <sub>3</sub> Films. ACS Applied Materials & Interfaces, 2017, 9, 27402-27408.	8.0	23

#	Article	IF	CITATIONS
109	Solvent regulation synthesis of single-component white emission carbon quantum dots for white light-emitting diodes. Nanotechnology Reviews, 2021, 10, 465-477.	5.8	23
110	Space-confined growth of monolayer ReSe2 under a graphene layer on Au foils. Nano Research, 2019, 12, 149-157.	10.4	22
111	Zone-Folded Longitudinal Acoustic Phonons Driving Self-Trapped State Emission in Colloidal CdSe Nanoplatelet Superlattices. Nano Letters, 2021, 21, 4137-4144.	9.1	22
112	Thermal conductivity of suspended single crystal CH <sub>3</sub> NH <sub>3</sub> Pbl <sub>3</sub> platelets at room temperature. Nanoscale, 2017, 9, 8281-8287.	5.6	20
113	The Auger process in multilayer WSe <sub>2</sub> crystals. Nanoscale, 2018, 10, 17585-17592.	5.6	20
114	Inner-Stress-Optimized High-Density Fe <sub>3</sub> O <sub>4</sub> Dots Embedded in Graphitic Carbon Layers with Enhanced Lithium Storage. ACS Applied Materials & Interfaces, 2020, 12, 15043-15052.	8.0	20
115	Strong Piezoelectricity in 3Râ€MoS <sub>2</sub> Flakes. Advanced Electronic Materials, 2022, 8, .	5.1	20
116	Near-infrared active metamaterials and their applications in tunable surface-enhanced Raman scattering. Optics Express, 2014, 22, 2989.	3.4	19
117	Monitoring of Changes in Composition of Soybean Oil During Deepâ€Fat Frying with Different Food Types. JAOCS, Journal of the American Oil Chemists' Society, 2016, 93, 69-81.	1.9	19
118	Boosting the electrocatalytic activity of amorphous molybdenum sulfide nanoflakes <i>via</i> nickel sulfide decoration. Nanoscale, 2019, 11, 22971-22979.	5.6	19
119	Salt-assisted growth and ultrafast photocarrier dynamics of large-sized monolayer ReSe2. Nano Research, 2020, 13, 667-675.	10.4	19
120	Inch-Scale Ball-in-Bowl Plasmonic Nanostructure Arrays for Polarization-Independent Second-Harmonic Generation. ACS Nano, 2021, 15, 1291-1300.	14.6	19
121	Effects of potassium alum addition on physicochemical, pasting, thermal and gel texture properties of potato starch. International Journal of Food Science and Technology, 2011, 46, 1621-1627.	2.7	18
122	The Growth of Ultralong ZnTe Micro/Nanostructures: The Influence of Polarity and Twin Direction on the Morphogenesis of Nanobelts and Nanosheets. Crystal Growth and Design, 2013, 13, 2590-2596.	3.0	18
123	Scattering focusing and localized surface plasmons in a single Ag nanoring. Applied Physics Letters, 2010, 97, .	3.3	17
124	Low Threshold Fabry–Pérot Mode Lasing from Lead Iodide Trapezoidal Nanoplatelets. Small, 2018, 14, e1801938.	10.0	17
125	Hyperbranched Microwire Networks of Organic Cocrystals with Optical Waveguiding and Lightâ€Harvesting Abilities. Angewandte Chemie - International Edition, 2021, 60, 27046-27052.	13.8	17
126	Temperature-dependent Raman spectroscopy studies of the interface coupling effect of monolayer ReSe <sub>2</sub> single crystals on Au foils. Nanotechnology, 2018, 29, 204003.	2.6	16

#	Article	IF	CITATIONS
127	Probing Far-Infrared Surface Phonon Polaritons in Semiconductor Nanostructures at Nanoscale. Nano Letters, 2019, 19, 5070-5076.	9.1	16
128	Photoluminescence properties of ultrathin CsPbCl3 nanowires on mica substrate. Journal of Semiconductors, 2019, 40, 052201.	3.7	16
129	Ultrafast Internal Exciton Dissociation through Edge States in MoS <sub>2</sub> Nanosheets with Diffusion Blocking. Nano Letters, 2022, 22, 5651-5658.	9.1	16
130	Surface State Mediated Interlayer Excitons in a 2D Nonlayered–Layered Semiconductor Heterojunction. Advanced Electronic Materials, 2017, 3, 1700373.	5.1	15
131	Charge-Transfer-Induced Photoluminescence Properties of WSe <sub>2</sub> Monolayer–Bilayer Homojunction. ACS Applied Materials & Interfaces, 2019, 11, 20566-20573.	8.0	15
132	Graphoepitaxy of Large Scale, Highly Ordered CsPbBr 3 Nanowire Array on Muscovite Mica (001) Driven by Surface Reconstructed Grooves. Advanced Optical Materials, 2020, 8, 2000743.	7.3	15
133	Golden hour for perovskite photonics. Photonics Research, 2020, 8, PP1.	7.0	15
134	Analysis of factors affecting traction energy consumption of electric multiple unit trains based on data mining. Journal of Cleaner Production, 2020, 262, 121374.	9.3	14
135	Direct measurement of coherent phonon dynamics in solution-processed stibnite thin films. Physical Review B, 2014, 90, .	3.2	13
136	Manipulating Nonlinear Emission and Cooperative Effect of CdSe/ZnS Quantum Dots by Coupling to a Silver Nanorod Complex Cavity. Scientific Reports, 2014, 4, 4839.	3.3	13
137	Mechanical transmission enables EMT cancer cells to drive epithelial cancer cell migration to guide tumor spheroid disaggregation. Science China Life Sciences, 2022, 65, 2031-2049.	4.9	13
138	Lasing from reduced dimensional perovskite microplatelets: Fabry-Pérot or whispering-gallery-mode?. Journal of Chemical Physics, 2019, 151, 211101.	3.0	12
139	Direct evidence of hydrogen interaction with carbon: C–H complex in semi-insulating GaN. Applied Physics Letters, 2020, 116, .	3.3	12
140	Vapor-Phase Living Assembly of π-Conjugated Organic Semiconductors. ACS Nano, 2022, 16, 3290-3299.	14.6	12
141	A model for predicting the creep-fatigue life under stepped-isothermal fatigue loading. International Journal of Fatigue, 2013, 55, 1-6.	5.7	11
142	Additiveâ€Assisted Growth of Scaled and Quality 2D Materials. Small, 2022, 18, e2107241.	10.0	11
143	Room-temperature Near-infrared Excitonic Lasing from Mechanically Exfoliated InSe Microflake. ACS Nano, 2022, 16, 1477-1485.	14.6	11
144	Engineering Near-Infrared Light Emission in Mechanically Exfoliated InSe Platelets through Hydrostatic Pressure for Multicolor Microlasing. Nano Letters, 2022, 22, 3840-3847.	9.1	11

#	Article	IF	CITATIONS
145	Research progress of low-dimensional metal halide perovskites for lasing applications. Chinese Physics B, 2018, 27, 114209.	1.4	10
146	High quality two-photon pumped whispering-gallery-mode lasing from ultrathin CdS microflakes. Journal of Materials Chemistry C, 2019, 7, 12869-12875.	5.5	8
147	Pattern-Selective Molecular Epitaxial Growth of Single-Crystalline Perovskite Arrays toward Ultrasensitive and Ultrafast Photodetector. Nano Letters, 2022, 22, 2948-2955.	9.1	8
148	Steppedâ€isothermal fatigue analysis of engine piston. Fatigue and Fracture of Engineering Materials and Structures, 2014, 37, 417-426.	3.4	7
149	Differences in Dry Sliding Wear Behavior between Al–12Si–CuNiMg Alloy and Its Composite Reinforced with Al2O3 Fibers. Materials, 2019, 12, 1749.	2.9	7
150	Intercalation-Mediated Synthesis and Interfacial Coupling Effect Exploration of Unconventional Graphene/PtSe <sub>2</sub> Vertical Heterostructures. ACS Applied Materials & Interfaces, 2019, 11, 48221-48229.	8.0	7
151	Effect of Fatigue Behavior on Microstructural Features in a Cast Al-12Si-CuNiMg Alloy Under High Cycle Fatigue Loading. Journal of Materials Engineering and Performance, 2013, 22, 3834-3839.	2.5	6
152	Taming excitons in Il–VI semiconductor nanowires and nanobelts. Journal Physics D: Applied Physics, 2014, 47, 394009.	2.8	6
153	Spontaneous formation and spatial self-organization of mechanically induced mesenchymal-like cells within geometrically confined cancer cell monolayers. Biomaterials, 2022, 281, 121337.	11.4	6
154	Ultrafast Antisolvent Growth of Single-Crystalline CsPbCl <sub>3</sub> Microcavity for Low-Threshold Room Temperature Blue Lasing. ACS Applied Materials & Interfaces, 2022, 14, 21356-21362.	8.0	6
155	Atomic structure and electrical/ionic activity of antiphase boundary in CH3NH3PbI3. Acta Materialia, 2022, 234, 118010.	7.9	6
156	Exciton–polaritons in semiconductors. Journal of Semiconductors, 2019, 40, 090401.	3.7	5
157	Advanced optical gain materials keep on giving. Science China Materials, 2020, 63, 1345-1347.	6.3	4
158	High-Temperature Dry Sliding Wear Behavior of Al–12Si–CuNiMg Alloy and its Al2O3 Fiber-Reinforced Composite. Metals and Materials International, 2021, 27, 3641-3651.	3.4	4
159	Millimeter-scale growth of highly ordered CsPbBr <sub>3</sub> single-crystalline microplatelets on SiO <sub>2</sub> /Si substrate by chemical vapor deposition. Journal Physics D: Applied Physics, 2021, 54, 334004.	2.8	4
160	Solar Cells: Synthesis of Organic-Inorganic Lead Halide Perovskite Nanoplatelets: Towards High-Performance Perovskite Solar Cells and Optoelectronic Devices (Advanced Optical Materials) Tj ETQq0 0 0 r	g <b>BT</b> 3/Over	ock 10 Tf 50
161	Software-defect prediction within and across projects based on improved self-organizing data mining. Journal of Supercomputing, 2022, 78, 6147-6173.	3.6	3

#	Article	IF	CITATIONS
163	Cyclic stress-assisted surface diffusion and stress concentration of machined surface topography. Engineering Fracture Mechanics, 2020, 234, 107087.	4.3	2
164	A novel software defect prediction approach using modified objective cluster analysis. Concurrency Computation Practice and Experience, 2021, 33, e6112.	2.2	2
165	Edge Raman enhancement at layered PbI <sub>2</sub> platelets induced by laser waveguide effect. Nanotechnology, 2022, 33, 035203.	2.6	2
166	Influence of intrinsic or extrinsic doping on charge state of carbon and its interaction with hydrogen in GaN. Applied Physics Letters, 2022, 120, .	3.3	2
167	Nanowire-Based Lasers. Nanostructure Science and Technology, 2019, , 367-393.	0.1	1
168	Analysis of multiple failure behaviors of steering knuckle ball hinge of multi-axle heavy vehicle. Advances in Mechanical Engineering, 2021, 13, 168781402110522.	1.6	1
169	Energy Consumption Analysis of High-Speed Trains under Real Vehicle Test Conditions. Journal of Advanced Transportation, 2022, 2022, 1-13.	1.7	1
170	Motion and Constraint Analysis Based on Screw Theory. , 2015, , .		0